AVE Trends in Intelligent Energy Letters

Performance Enhancement of Grid-Connected PV System Using Re-Boost Converter with PI and FOPID Controlled Inverter

Srinivas Kandadai Nagaratnam[1], K. Arulvendhan[2], P. Srinivasan[3,*], C. Sathish Kumar[4], Saly Jaber[5]

[1,2]Department of Electrical and Electronics Engineering, SRM Institute of Science and Technology, Ramapuram, Chennai, Tamil Nadu, India.
[3]Department of Electrical and Electronics Engineering, Saveetha Engineering College, Thandalam, Chennai, Tamil Nadu, India.
[4]Department of Computer Science, Faculty of Science and Humanities, SRM Institute of Science and Technology, Ramapuram, Chennai, Tamil Nadu, India.
[5]Department of Analytical Chemistry, Saint Joseph University, Beirut, Lebanon.
srinivak@srmist.edu.in[1], arulvenk@srmist.edu.in[2], srinivasp808@gmail.com[3], sathishc@srmist.edu.in[4], saly.jaber@usj.edu.lb[5]

*Corresponding author

Abstract: This Paper targets the analysis and optimization of the dynamic time response of a photovoltaic (PV) energy conversion system with a closed-loop re-boost converter, with active and reactive power control implemented by a fractional-order proportional–integral–derivative (FOPID) controller. The research targets the modelling and simulation of FOPID-based current limitation for a grid-connected inverter, ensuring stable and efficient operation under varying load and grid conditions. Active and reactive power control have played major roles in power system applications, especially with voltage-source inverters (VSIs), where pulse-width modulation (PWM) techniques are used to generate the switching pulses. To improve power quality, an active filter is employed to eliminate load current harmonics, ensuring the overall reliability of the grid interface. Simulation experiments are performed to compare the responses of FOPID-controlled active and reactive power methods with those of a conventional proportional–integral (PI) controller. The comparison is based on extensive time-domain parameters and includes data on transient response, settling time, and harmonic suppression. Comparative results indicate that although both control schemes are satisfactory, the FOPID-based scheme consistently delivers better performance, with higher dynamic response, lower overshoot, and improved harmonic elimination than its PI-based counterpart.

Keywords: Re-Boost Converter; Solar Panel; Pulse Width Modulation; PWM Inverter; PI-Controller; FOPID-Controller; Voltage Source Inverters; Grid-Connected PV Systems.

Cite as: S. K. Nagaratnam, K. Arulvendhan, P. Srinivasan, C. S. Kumar, and S. Jaber, "Performance Enhancement of Grid-Connected PV System Using Re-Boost Converter with PI and FOPID Controlled Inverter," *AVE Trends in Intelligent Energy Letters*, vol. 1, no. 2, pp. 87–99, 2025.

Journal Homepage: https://www.avepubs.com/user/journals/details/ATIEL

Received on: 14/11/2024, **Revised on:** 02/01/2025, **Accepted on:** 13/02/2025, **Published on:** 09/12/2025

DOI: https://doi.org/10.64091/ATIEL.2025.000188

1. Introduction

One of the most promising and sustainable solutions to the increasing energy demand of the modern man has come in the form of solar power generation, where, in countries around the world, the demands placed on traditional sources of energy lead to greater atmospheric concerns and greater environmental implications. The ever-decreasing supply of conventional energy resources, the continually rising electricity generation costs, and the urgent problem of greenhouse gas emissions make solar photovoltaic (PV) technology a viable, sustainable, and efficient alternative energy source. In many areas, especially in the developing world, solar power is increasingly seen as more than just a way for developing countries to supplement conventional power plants; to some, it is an essential technology for electrifying rural and remote areas that centralised power plants do not reach or serve [1]. Under these settings, the importance of PV power conversion systems is crucial, as they affect the reliability, quality, and energy efficiency delivered to residential and industrial loads. States such as Gujarat in India have proven the grand-scale feasibility of solar generation by harnessing abundant solar radiation to convert sunlight directly into electricity, with no chemical emissions. Nevertheless, the efficient deployment of solar power production still faces challenges, including the intermittency of the solar resource, the temperature dependence of PV modules, and the need for power conditioning stages to be connected to the grid and to function correctly under all operating conditions [2].

The Sunlight converted to electrical power undergoes multiple steps, and in a grid-integrated system, an efficient Power conditioner is required for Power control, regulation, and power flow optimisation. For that purpose, depending on the application, they can be designed in single-stage (SS) or two-stage (TS) topologies, each with Pros and Cons. At the residential scale, single-stage power conditioners are commonly used because their structure is relatively simple and low-cost, and their performance is sufficient for power levels typically below 5 kW [3]. A conventional method used herein is a single-phase PWM inverter for connecting PV modules directly to the grid. The high intrinsic efficiency and power density are significant as well, helping reduce costs and enabling use for small, decentralised solar installations at homes and small businesses. However, the single-stage structure typically lacks galvanic isolation because no transformer is used between the PV modules and the grid, posing safety risks under certain circumstances. Furthermore, the inverter must invert the DC voltage generated by the PV modules into alternating current (AC) that can be fed to the grid and must also perform maximum power point tracking (MPPT) to ensure the PV system continuously operates at its maximum power point. To achieve such dual functionality while retaining stability and efficiency constitutes a fundamental technical challenge [4]; [5].

To achieve high efficiency and high-frequency operations, resonant components are explored as substitutes. For example, resonant-type converters can be realised in ZCS or ZVS mode, reducing switch losses and EMI and enabling high-frequency DC–DC conversion. Such converters are particularly advantageous in PV applications where high-frequency operation may be required to achieve a compact design and a fast dynamic response [6]. Nevertheless, resonant converters generally require additional passive components, such as inductors and capacitors, which can increase circuit complexity, overall volume, and even price. Furthermore, the rating of the converter components shall closely match the requirements for output voltage and current, thereby reducing the need to scale up these components in larger plants. Two-stage architectures offer an alternative, particularly when performance and flexibility requirements are stronger. Usually, a two-stage system consists of a DC–DC converter cascaded with a DC–AC inverter, with a DC link capacitor serving as an energy buffer between them. The DC–DC converter can be a transformerless, non-isolated, medium voltage DC–DC converter or have galvanic isolation using a high frequency transformer [7]. Non-isolated topologies are usually more efficient but better suited to low-voltage residential applications, while isolated topologies improve safety and offer voltage-levelling flexibility at the expense of efficiency. In such systems, the DC–DC converter performs voltage regulation and MPPT independently, allowing the inverter to focus on synchronisation and grid power delivery [8].

This separation of functions enhances control precision and flexibility, but it comes at the expense of additional components and higher cost. While two-stage systems provide robust performance, their practical implementation in small-scale residential PV plants introduces challenges. Because the power levels are relatively low (often below 3 kW), only a limited number of PV modules can be connected in series to form a string [9]. Consequently, the inverter input DC voltage may fall below the required level for direct DC–AC conversion, particularly when PV module temperatures rise above 40–45 °C, reducing the module voltage output. To overcome this limitation, a step-up DC–DC converter is often placed between the PV array and the inverter to boost the input voltage, thereby ensuring reliable operation and enabling MPPT [10]. Although effective, this additional stage increases system complexity, size, and cost, prompting researchers to explore improved single-stage configurations with built-in voltage boosting. Among these alternatives, single-stage converters with internal voltage boosting, such as flying inductor converters or hybrid topologies combining elements of single- and two-stage systems, have attracted attention [11]. For instance, quasi-sine-wave PWM inverters with time-sharing can selectively activate a boost converter stage only when the input voltage is insufficient to generate the required grid voltage.

Such designs achieve a quasi-single-step operation, optimising efficiency while ensuring reliable grid connection even under low PV voltage conditions. Similarly, in battery-assisted applications, DC–DC converters may regulate the output voltage to levels close to the input voltage, ensuring stability and continuity of power supply during fluctuations in solar generation [12]. To increase efficiency and minimise component loading, the concept of series compensation has been proposed. In this method,

the buck-boost DC–DC converter is used in cascade with the PV strings, not in parallel. The converter only corrects for the voltage mismatch between the PV output and the inverter input, not the entire power. This greatly decreases the converter's power rating, reduces losses, and improves efficiency while ensuring stable operation. The converter's function is reduced when the PV output voltage is high enough to operate the inverter, thereby further improving the system's performance. Moreover, such designs enable the integration of chargeable and dischargable batteries that can deliver device power to the system during low irradiance and/or disruptions to the system for any reason [13]. The series-compensation-based converter systems according to the invention are particularly suited for residential and suburban use, where economic, small size, and reliability are important factors. They embody the advantages of voltage gain, MPPT capability, and low converter stress, without compromising overall efficiency and power quality. The increasing penetration of such systems is also in line with the electrification of distributed solar power generation.

2. Methodology

The methodology adopted for this work is based on the modelling, control, and performance analysis of a grid-connected photovoltaic (PV) system integrated with a re-boost converter, an inverter, and advanced control schemes, as shown in Figure 1. The block diagram, which highlights the flow of power from the PV array and battery through the re-boost converter and inverter to the grid, while the controllers ensure stability, power quality, and dynamic performance.

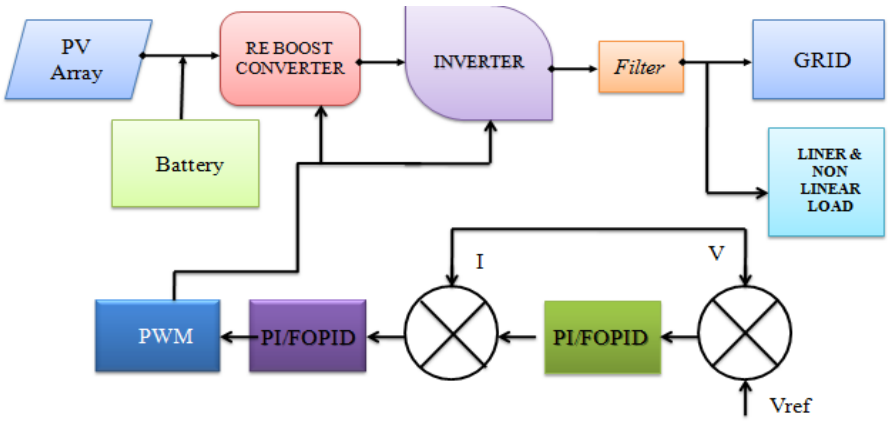

Figure 1: Block diagram of PV and battery-based re-boost converter with inverter in a closed-loop grid-connected system with PI and FOPID controller

2.1. Photovoltaic Cell

The system begins with the PV module, which acts as the primary energy source. A PV cell operates on the principle of the photovoltaic effect, where sunlight is directly converted into electrical energy. The equivalent electrical circuit of a PV cell can be modelled as a current source in parallel with a diode, accounting for the photocurrent generated by solar irradiation and the diode current due to recombination losses (Figure 2).

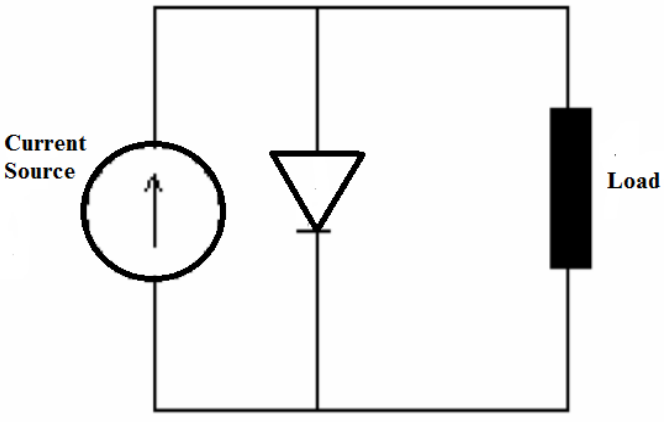

Figure 2: Equivalent circuit of solar panel

Load current:

$$I_L = I_{ph} - I_D \quad (1)$$

Where I_L is the load current, Iph is the photo current, and ID is the diode current. Voltage and current vary with solar irradiance and temperature. As both voltage and current vary with environmental conditions, the PV module inherently exhibits nonlinear power characteristics, necessitating a maximum power point tracking (MPPT) algorithm to extract optimal energy at all times.

2.2. Maximum Power Point Tracking (MPPT)

The MPPT algorithm is integrated with the re-boost converter to achieve optimal energy harvesting. The principle behind MPPT is based on the maximum power transfer theorem, which states that the output power of a system is maximised when the source and load impedances are matched. In the PV system, this translates to dynamically adjusting the PV array's operating voltage and current to maximise the product P = V × I under varying irradiation and temperature conditions. The MPPT controller generates the reference signal that regulates the duty cycle of the re-boost converter, ensuring that the converter operates at the most efficient point on the PV characteristic curve.

2.3. Re-Boost Converter

The re-boost converter serves as an essential power conditioning stage in the system. Unlike a simple boost converter, the re-boost topology allows for flexible voltage regulation by stepping up the DC voltage from the PV array to the required level for the inverter input. It is a high-frequency switching circuit comprising an inductor, a controlled switch, diodes, and a capacitor.

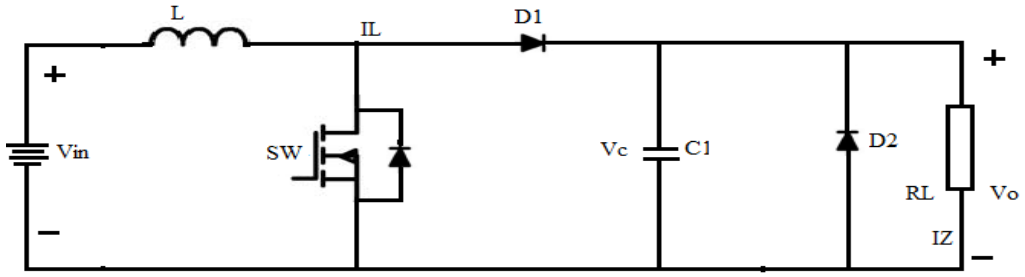

Figure 3: Re-boost converter

The duty cycle of a re-boost converter controlling the switching signal depends on the input voltage for the output voltage. Values for the passive components, particularly the inductor and capacitor, are selected based on the required output-voltage ripple, the constant switching frequency, and the current-ripple constraints. Then, steady-state operation is guaranteed, with losses and efficiency reduced to a minimum. The circuit diagram of the Re-boost converter is shown in Figure 3. The conditioned DC voltage from the re-boost converter is fed to an inverter that generates AC power for grid connection. A filter is connected at the inverter's output to avoid harmonics and ensure power quality, which must be met before connecting to the grid. The system handles linear and nonlinear loads, and it is known that, to maintain stability under these conditions, advanced control strategies (PI and FOPID) are used. These controllers regulate the active and reactive power flow between the inverter and the grid to improve dynamic response and reduce steady-state error. The control system is implemented in a closed-loop architecture, with the measured voltage and current compared to the preset reference levels. These error signals are applied to the PI-FOPID controller that implements the desired linear region, yielding control signals for the PWM unit. The PWM controls the re-boost converter and inverter, turning them on and off to ensure the system tracks the reference inputs. The fractional-order terms of the proposed FOPID controller improve robustness and provide better transient and steady-state performance, as shown in the simulation results compared with the standard PI controller. Thus, the methodology integrates three key aspects: accurate modelling of the PV module, efficient DC–DC conversion via a re-boost converter with MPPT control, and precise regulation of grid power flow using advanced controllers. Together, these ensure reliable energy harvesting, reduced harmonics, lower steady-state error, and improved response time, making the system suitable for real-world grid-connected PV applications:

$$V_o = \frac{V_s}{1-D} \quad (2)$$

The output voltage (V_o) depends on the input voltage (Vs) and the duty cycle (D). The standards for inductors and capacitors can be designed using the equations below, selecting a constant switching frequency (f), and specifying the (ΔVo/Vo) output voltage ripple appropriately:

$$C = \frac{D}{R\left(\frac{\Delta V_o}{V_o}\right)f} \quad (3)$$

$$L = \frac{D(1-D)^2 R}{2f} \quad (4)$$

3. Simulation Discussion and Experimental Results

The simulation model of the PV array integrated with the re-boost converter, inverter, and grid-connected load under disturbance conditions is illustrated in Figure 4.

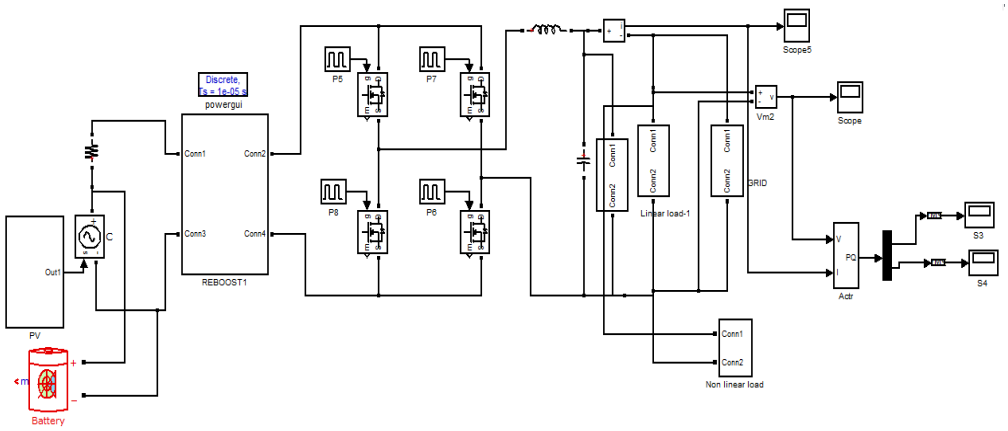

Figure 4: Circuit diagram of PV and battery-based Re-boost converter with an inverter grid-connected load disturbance system

The voltage response of the PV module is shown in Figure 5, where the steady-state output voltage is approximately 48 V.

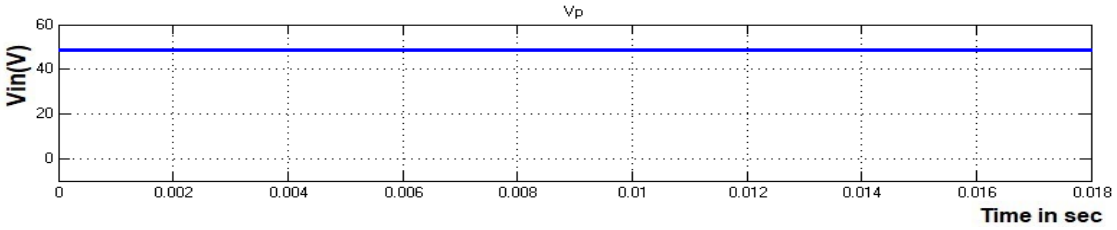

Figure 5: Voltage across PV

The output voltage of the re-boost converter is shown in Figure 6, with an amplified value of approximately 140 V.

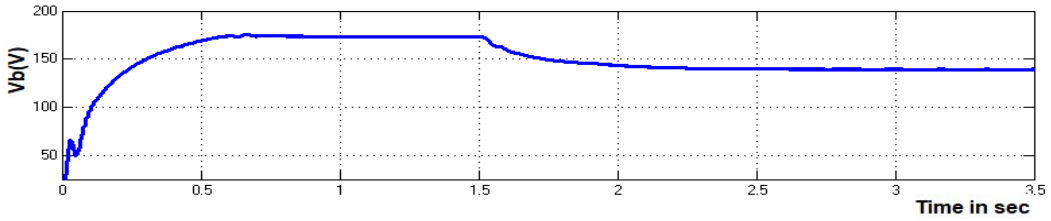

Figure 6: Voltage across the re-boost converter

Figure 7 depicts the voltage profile across the RL load, which stabilises at nearly 200 V.

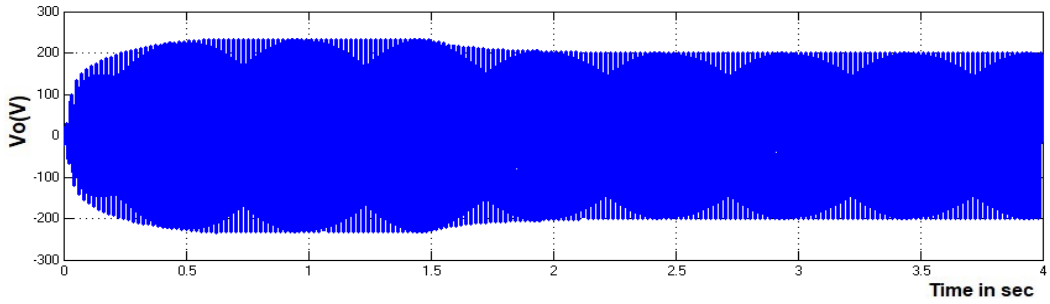

Figure 7: Voltage across RL load

The quality of the output voltage is further evaluated using total harmonic distortion (THD) analysis, as presented in Figure 8.

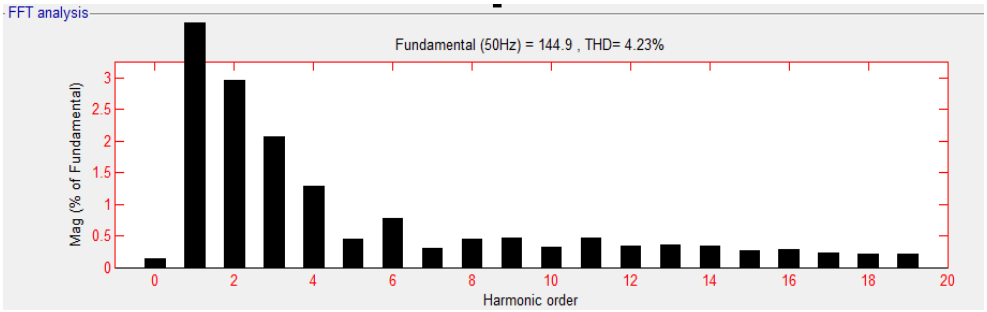

Figure 8: Output voltage THD

The fundamental component at 50 Hz is recorded as 144.9, with a corresponding THD percentage of 4.23%. The current through the RL load is shown in Figure 9, reaching 10 A under the given operating conditions.

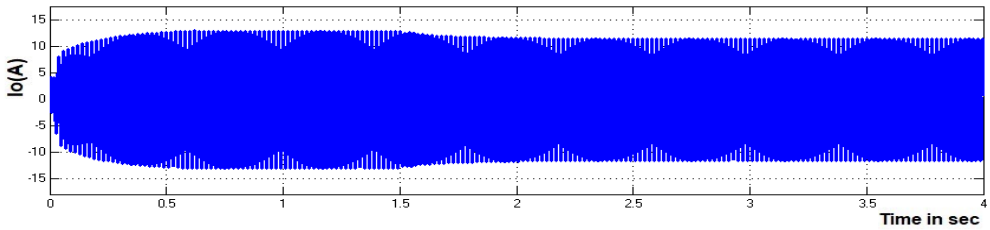

Figure 9: Current through RL load

The harmonic profile of the load current is depicted in Figure 10, where the fundamental current component at 50 Hz is 11.16 A, and the associated THD is calculated as 4.56%.

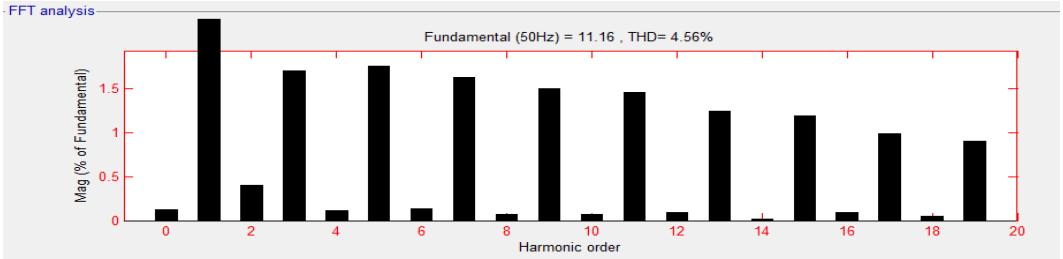

Figure 10: Output current THD

The system's power analysis is presented in Figures 11 and 12. The real power delivered to the grid is approximately 140 W, while the reactive power component is approximately 1000 VAR.

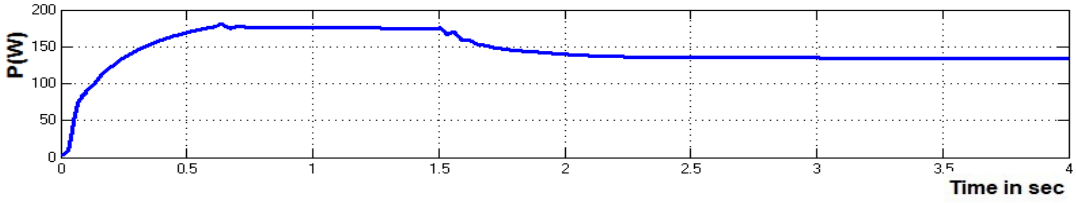

Figure 11: Real power

These results confirm that the proposed PV, re-boost converter inverter configuration effectively regulates the voltage and current while maintaining harmonic levels within acceptable limits, thereby ensuring stable power delivery to the grid under load disturbances.

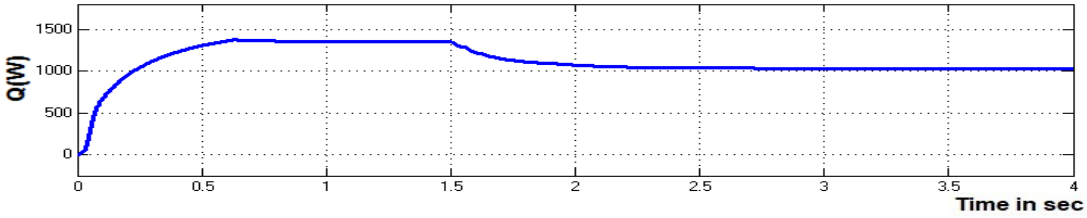

Figure 12: Reactive power

The configuration of the PV array integrated with the re-boost converter, inverter, and grid connection operating under a closed-loop PI controller is presented in Figure 13.

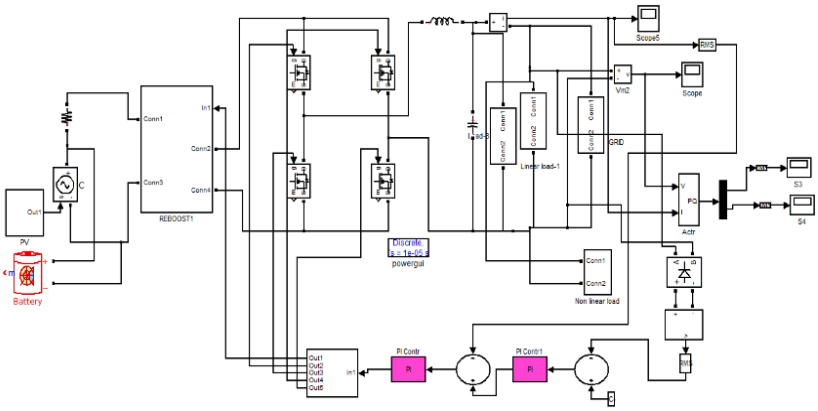

Figure 13: Circuit diagram of PV and battery-based re-boost converter with inverter grid-connected closed-loop PI-PI controller

The voltage characteristic of the PV module is shown in Figure 14, where the output voltage is approximately 50 V.

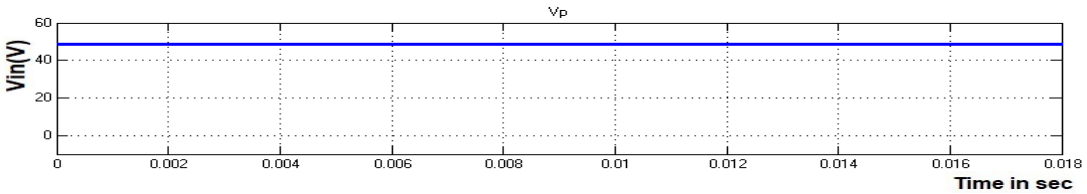

Figure 14: Voltage across PV

The boosted voltage at the output of the re-boost converter is shown in Figure 15, with a recorded value of about 175 V.

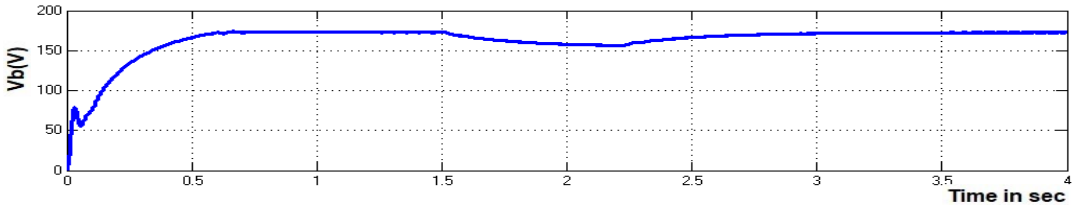

Figure 15: Voltage across the re-boost converter

Figure 16 displays the voltage across the RL load, which stabilises at nearly 230 V.

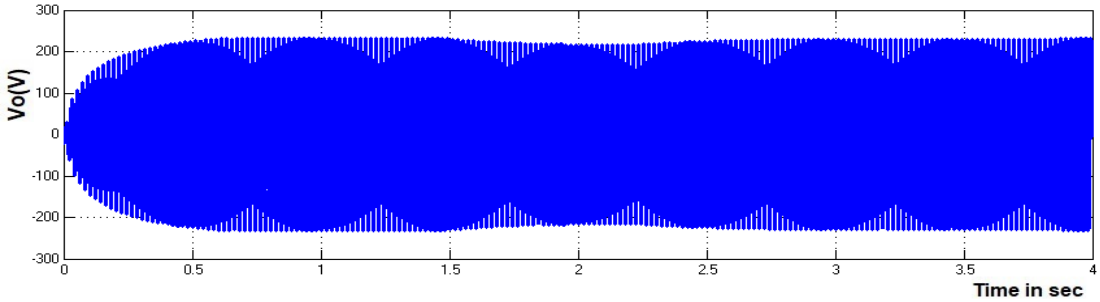

Figure 16: Voltage across the RL load

The harmonic performance of the output voltage is analysed in Figure 17, where the fundamental component at 50 Hz is 122.2, and the corresponding total harmonic distortion (THD) is 3.36%.

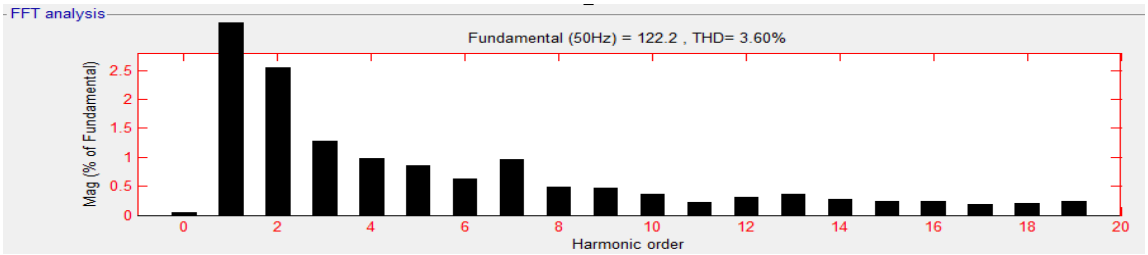

Figure 17: Output voltage THD

The current through the RL load is shown in Figure 18, reaching approximately 12.5 A.

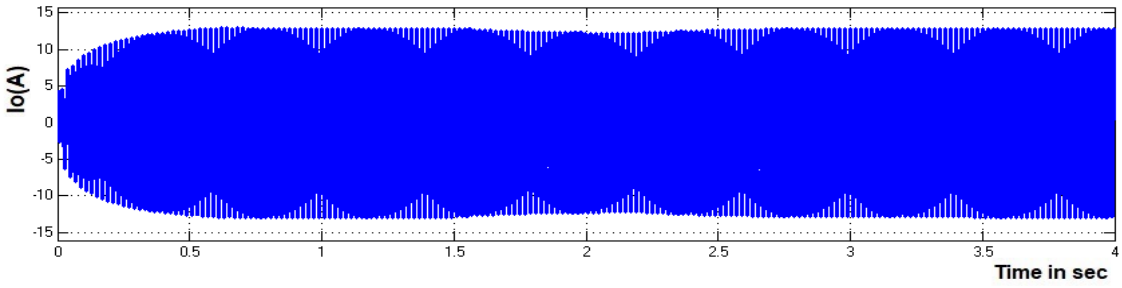

Figure 18: Current through RL load

Figure 19 presents the current harmonic spectrum, with the fundamental component at 50 Hz measured as 11.52 A and a THD value of 3.92%.

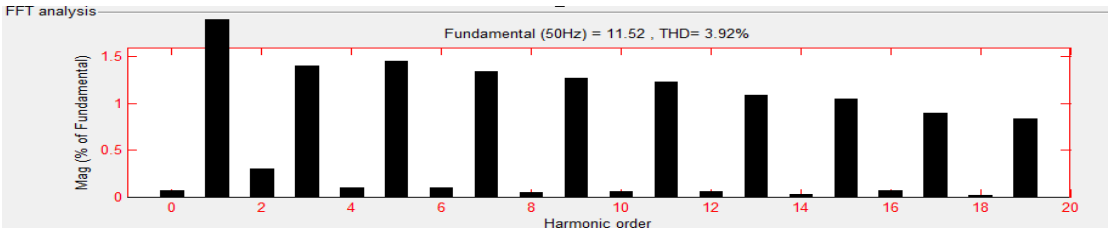

Figure 19: Output current THD

The system's power characteristics are summarised in Figures 20 and 21. The real power output is approximately 175 W, while the reactive power is approximately 1400 VAR.

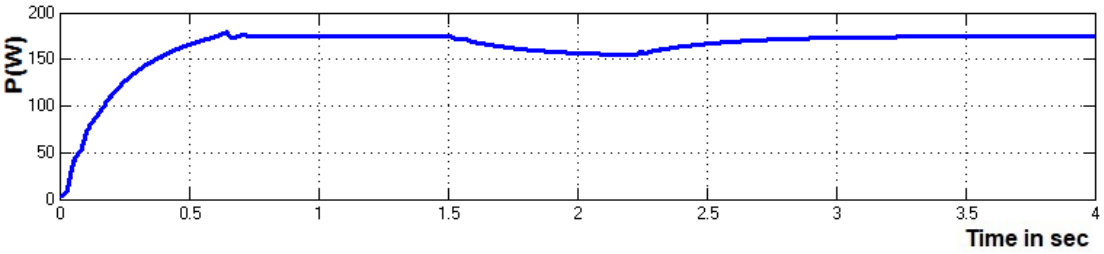

Figure 20: Real power flow

These findings show that the PV-re-boost converter–inverter system regulated by a PI controller can maintain stable voltage and current levels, deliver adequate real power, and reduce harmonic distortion within permissible limits for grid-connected operation.

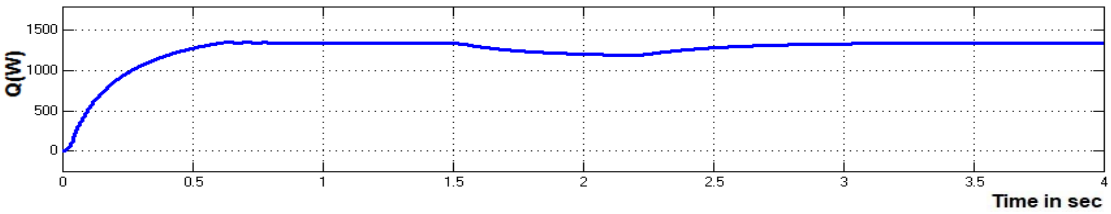

Figure 21: Reactive power flow

The operation of the PV array integrated with the re-boost converter and inverter under a grid-connected closed-loop FOPID controller is illustrated in Figure 22.

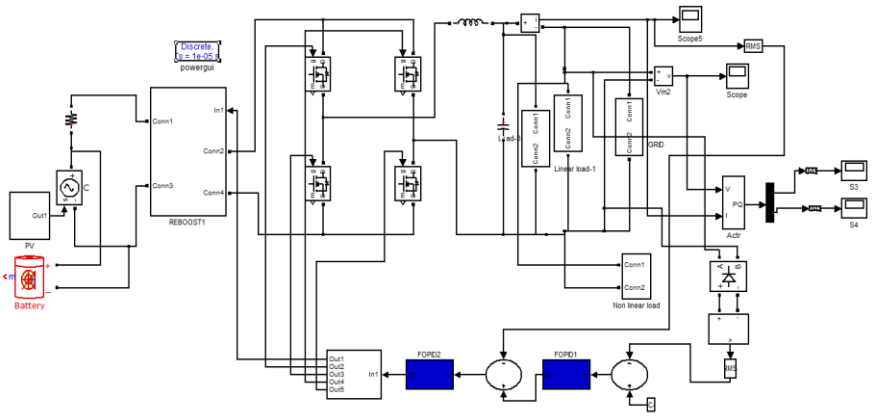

Figure 22: Circuit diagram of PV and battery-based Re boost converter with inverter grid-connected closed-loop FOPID-FOPID controller

The voltage profile of the PV module is presented in Figure 23, showing a stable output of approximately 50 V.

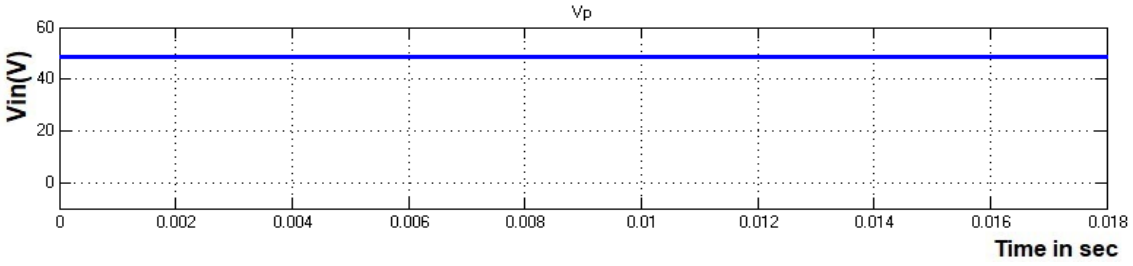

Figure 23: Voltage across PV

The boosted voltage obtained from the re-boost converter is displayed in Figure 24, where the output reaches about 175 V.

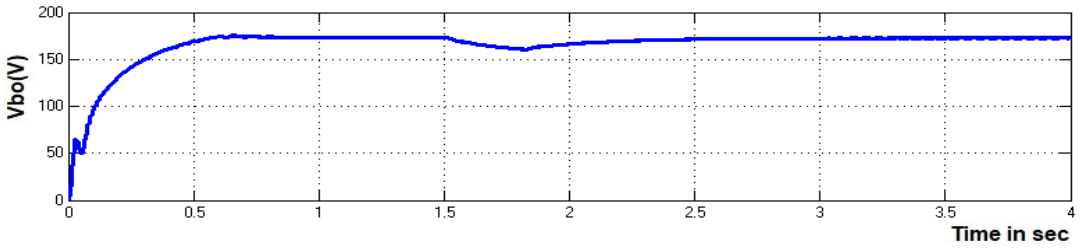

Figure 24: Voltage across the re-boost converter

The corresponding voltage across the RL load is shown in Figure 25 and is maintained at nearly 230 V.

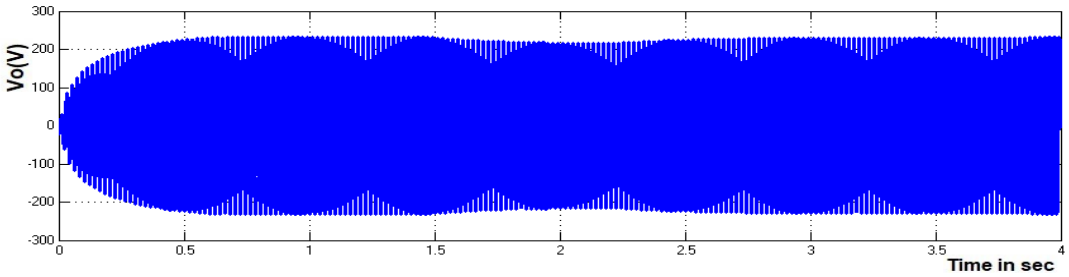

Figure 25: Voltage across RL load

The harmonic quality of the output voltage is analysed in Figure 26, with the fundamental component at 50 Hz measured as 152.7 and the total harmonic distortion (THD) recorded at 2.92%.

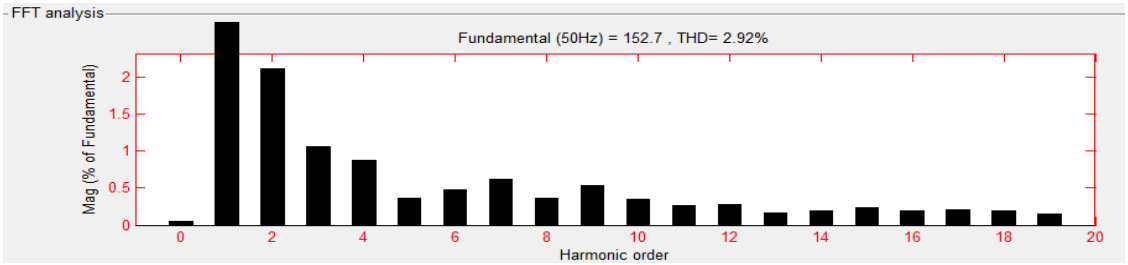

Figure 26: Output voltage THD

The current through the RL load is shown in Figure 27 and is 12.5 Amps.

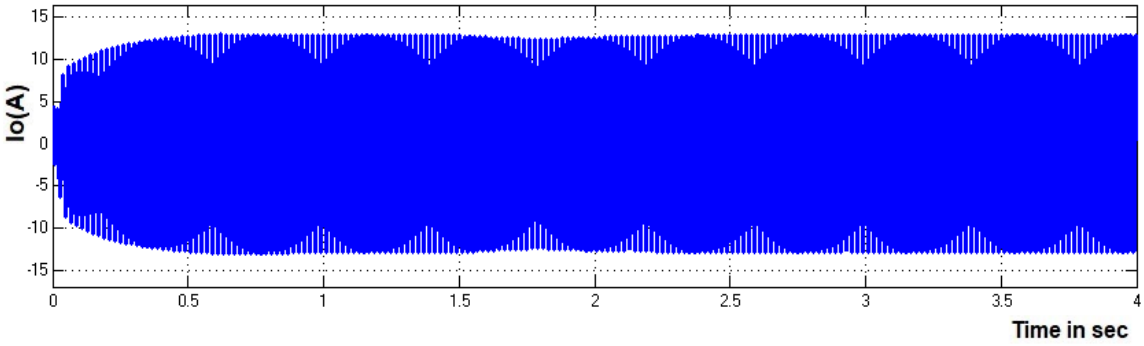

Figure 27: Current through RL load

Current THD is shown in Figure 28. The current THD fundamental at 5Hz is 11.96, and the THD is 3.22%.

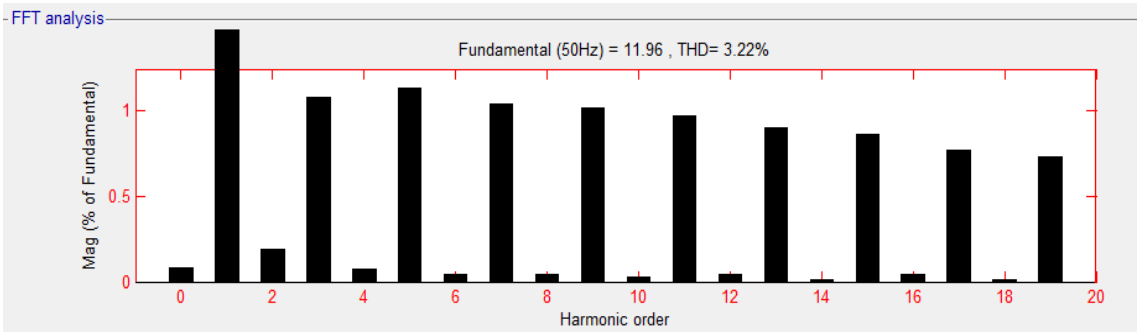

Figure 28: Output current THD

The real power is shown in Figure 29 and is 175 VAR.

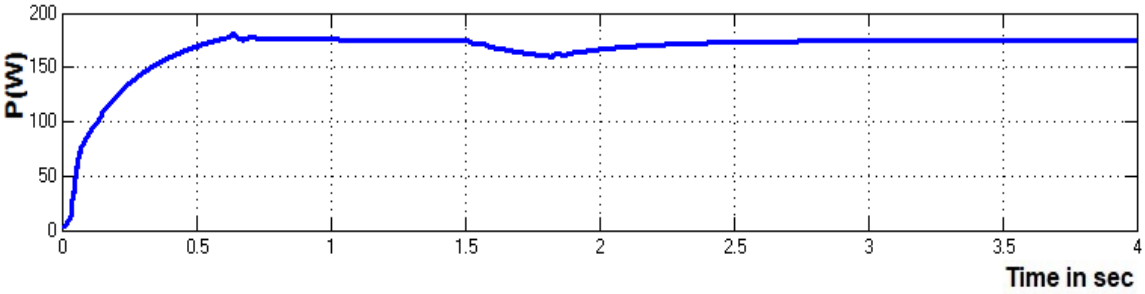

Figure 29: Real power

The reactive power is shown in Figure 30 and is 1400 watts.

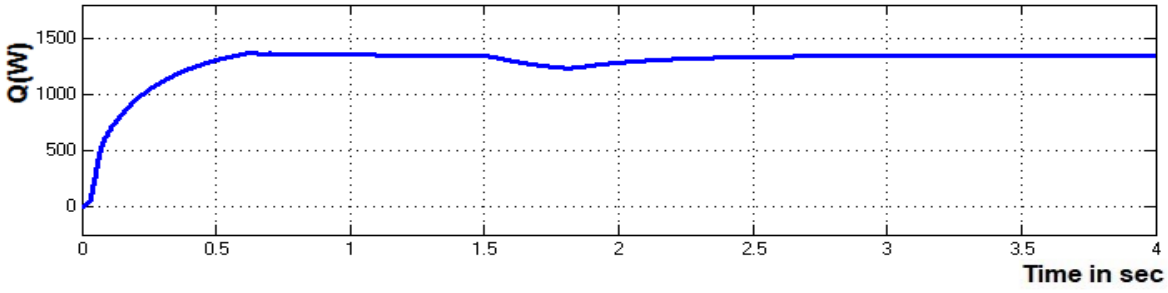

Figure 30: Reactive power

The comparative evaluation of time-domain parameters for the PI and FOPID controllers is presented in Table 1. The application of the FOPID–FOPID scheme results in significant performance improvements. Specifically, the rise time decreases from 1.64 s to 1.57 s, while the peak time is reduced from 2.21 s to 1.82 s. Similarly, the settling time shows improvement, dropping from 2.67 s to 2.04 s.

Table 1: Comparison of time domain parameters

Controller	$T_{r(sec)}$	$T_{s(sec)}$	$T_{p(sec)}$	$E_{ss(V)}$
PI	1.64	2.67	2.21	3.3
FOPID	1.57	2.04	1.82	2.4

In addition, the steady-state error decreases notably, from 3.5 V in the PI–PI case to 2.4 V with the FOPID–FOPID approach. These enhancements highlight the superior dynamic response of the FOPID controller compared to the conventional PI method. The comparison is illustrated in the bar chart of time-domain parameters in Figure 31, which clearly demonstrates the improvements achieved by the proposed control strategy.

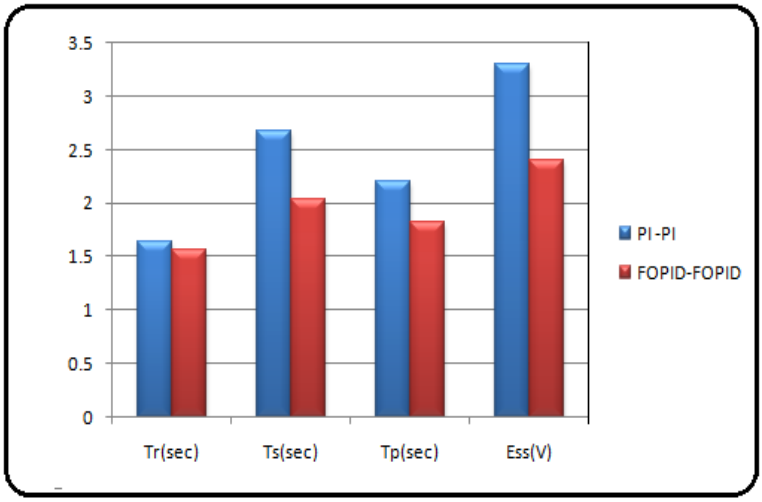

Figure 31: Bar chart comparison of crime parameters

The comparative analysis of voltage and current total harmonic distortion (THD) is summarised in Table 2. For the PI controller, the voltage THD is 3.60%, and the current THD is 3.92%. In contrast, the FOPID controller demonstrates improved performance, with voltage THD reduced to 2.92% and current THD lowered to 3.22%. These results clearly indicate that the FOPID-based system provides superior harmonic suppression compared to the conventional PI-controlled approach.

Table 2: Comparison of voltage and current THD

Controller	Voltage THD	Current THD
PI	3.60%	3.92%
FOPID	2.92%	3.22%

4. Conclusion

The performance evaluation of the re-boost converter-based active and reactive filter in a closed-loop grid-connected voltage source inverter demonstrates the effectiveness of the proposed control strategy. Simulation outcomes confirm that replacing the conventional PI controller with the FOPID controller yields noticeable improvements in both transient and steady-state performance. The steady-state error, initially observed at 3.5 V with PI control, is reduced to 2.6 V with FOPID control, indicating improved voltage regulation accuracy. Similarly, the settling time is reduced from 2.67 seconds to 2.04 seconds, highlighting the system's enhanced dynamic response. In addition to these improvements, the proposed design helps minimise total harmonic distortion (THD) of voltage and current, line voltage drop, and overall system error, thereby improving the quality of power delivered to the grid. Although the system offers these advantages, it has the drawback of requiring larger passive components, such as inductors and capacitors, which may increase size, cost, and complexity. Nonetheless, the trade-off appears justified in applications where improved performance and reliability are of higher priority. Overall, the study

suggests that the FOPID-based active and reactive filter is a strong alternative to existing PI-based systems, providing superior power quality, faster response, and greater robustness for grid-integrated renewable energy conversion systems.

Acknowledgement: The authors acknowledge the academic support, guidance, and facilities provided by SRM Institute of Science and Technology, Saveetha Engineering College and Saint Joseph University, which contributed to the successful completion of this work.

Data Availability Statement: This study uses a dataset on the performance enhancement of a grid-connected photovoltaic system using a re-boost converter with PI- and FOPID-controlled inverters.

Funding Statement: No external financial support was received for conducting the research or preparing the manuscript.

Conflicts of Interest Statement: The authors declare that there are no conflicts of interest, and all referenced materials have been appropriately cited.

Ethics and Consent Statement: Ethical clearance was obtained, and informed consent was secured from the relevant organizations and individual participants during the data collection process.

References

1. T. Yuvaraj, K. R. Devabalaji, J. A. Kumar, S. B. Thanikanti, and N. I. Nwulu, "A Comprehensive Review and Analysis of the Allocation of Electric Vehicle Charging Stations in Distribution Networks," *in IEEE Access*, vol. 12, no. 1, pp. 5404-5461, 2024.
2. M. P. Suresh, S. J. Isac, M. Joly, and J. A. Kumar, "Automatic fault detection and stability management using intelligent hybrid controller," *Electric Power Systems Research*, vol. 238, no. 1, p. 111075, 2025.
3. H. Mao, O. Abdel–Rahman, and I. Batarseh, "Active resonant tank to achieve zero voltage switching for non-isolated DC-DC converters with synchronous rectifiers," *in Proc. 31st Annual Conference of IEEE Industrial Electronics Society, 2005. IECON 2005*, Raleigh, North Carolina, United States of America, 2005.
4. A. Kotsopoulos and D. G. Holmes, "Performance of a series –parallel resonant DC-DC converter module for high current low voltage applications," *in proc. International Conference on Power Electronic Drives and Energy Systems for Industrial Growth, 1998*, Perth, Western Australia, Australia, 1998.
5. S. B. Kjaer, J. K. Pedersen, and F. Blaabjerg, "A Review of Single-Phase Grid-Connected Inverters for Photovoltaic Modules," *IEEE Trans. On Industrial Applications*, vol. 41, no. 5, pp. 1292–1306, 2005.
6. R. O. Caceres and I. Barbi, "A boost DC-AC converter, analysis, design and experimentation," *IEEE Trans. On Power Electronics*, vol. 14, no. 1, pp. 134–141, 1999.
7. K. Ogura, T. Nishida, E. Hiraki, M. Nakaoka, and S. Nagai, "Timesharing Boost Chopper Cascaded Dual Mode Single-phase Sine wave Inverter for Solar Photovoltaic Power Generation System," *in Proc. Of 35th Annual IEEE Power Electronics Specialists Conference*, Aachen, Germany, 2004.
8. J. Itoh and T. Fujii, "A New Approach for High Efficiency Buck-Boost DC/DC Converters Using Series Compensation," *in Proc. of IEEE Power Electronics Specialists Conference*, Rhodes, Greece, 2008.
9. G. Guidi, T. M. Undeland, and Y. Hori, "An Interface Converter with Reduced VA Ratings for Battery-Super Capacitor Mixed Systems," *IEEE PCC2007*, Nagoya, Japan, 2007.
10. J. H. R. Enslin and D. B. Snyman, "Combined Low-Cost, High-Efficient Inverter, Peak Power Tracker and Regulator for PV Applications," *IEEE Trans. On Power Electronics*, vol. 6, no. 1, pp. 73 – 82, 1991.
11. J. H. R. Enslin, J. D. V. Wyk, P. V. Rhyn, and J. J. Schoeman, "Development and characteristics of battery-fed, high power high-frequency converters in parallel operation," *in Proc. 2nd European Conf. Power Electronics and Applications, EPE-87*, Grenoble, France, 1987.
12. S. -J. Kim and S. -K. Sul, "A novel filter design for suppression of high voltage gradient in voltage-fed PWM inverter," *in Proc. IEEE Appl. Power Electron. Conf.*, Atlanta, Georgia, United States of America, 1997.
13. I. B. Huang and W. S. Lin, "Harmonic Reduction in Inverters by Use of Sinusoidal Pulse width Modulation," *IEEE Trans. On Industrial Electronics and Control Instrumentation*, vol. IECI-27, no. 3, pp. 201 - 207, 1980.